Virology 281, 109–116 (2001)
doi:10.1006/viro.2000.0778, available online at http://www.idealibrary.com on IDEAL®

Role of Distal Zinc Finger of Nucleocapsid Protein in Genomic RNA Dimerization of Human Immunodeficiency Virus Type 1; No Role for the Palindrome Crowning the R-U5 Hairpin

Michael Laughrea,*,†,[1] Ni Shen,*,† Louis Jetté,* Jean-Luc Darlix,§ Lawrence Kleiman,*,† and Mark A. Wainberg*,‡

*McGill AIDS Centre, Lady Davis Institute for Medical Research, Jewish General Hospital, and †Department of Medicine and ‡Department of Microbiology & Immunology, McGill University, Montreal, Quebec, Canada H3T 1E2; and §LaboRetro, Unité de Virologie Humaine, INSERM U412, Ecole Normale Supérieure de Lyon, 6934 Lyon Cedex, France

Received August 8, 2000; returned to author for revision September 23, 2000; accepted December 4, 2000

Genomic RNA isolated from HIV-1 variously mutated in nucleocapsid protein (NC) was characterized by nondenaturing gel electrophoresis. Mutations in the C-terminal, the N-terminal, and the linker regions had no effect on genomic RNA dimerization [they are R7R10K11S, P31L, R32G, S3(32–34), and K59L], while a C36S/C39S mutation in the distal zinc knuckle (Cys-His box or zinc finger) inhibited genome dimerization as much as disrupting the kissing-loop domain. The four mutations which inhibited $tRNA_{Lys3}$ genomic placement (i.e., the *in vivo* placement of $tRNA_{Lys3}$ on the primer binding site) had no effect on genome dimerization. Among five mutations which inhibited genome packaging, four had no effect on genome dimerization. Thus the N-terminal and linker regions of NC control genome packaging/$tRNA_{Lys3}$ placement (two processes which do not require mature NC) but have little influence on genome dimerization and 2-base extension of $tRNA_{Lys3}$ (two processes which are likely to require mature NC). It has been suggested, based on electron microscopy, that the AAGCUU82 palindrome crowning the R-U5 hairpin stimulates genomic RNA dimerization. To test this hypothesis, we deleted AGCU81 from wild-type viruses and from viruses bearing a disrupted kissing-loop hairpin or kissing-loop domain; in another mutant, we duplicated AGCU81. The loss of AGCU81 reduced dimerization by 2.5 ± 4%; its duplication increased it by 3 ± 6%. Dissociation temperature was left unchanged. We reach two conclusions. First, the palindrome crowning the R-U5 hairpin has no impact on HIV-1 genome dimerization. Second, genomic RNA dimerization is differentially influenced by NC sequence: it is Zn finger dependent but independent of the basic nature of the N-terminal and linker subdomains. We propose that the NC regions implicated in 2-base extension of $tRNA_{Lys3}$ are required for a second (maturation) step of tRNA placement. Genome dimerization and mature tRNA placement would then become two RNA–RNA interactions sharing similar NC sequence requirements.

Key Words: nucleocapsid protein; R-U5 hairpin; genomic RNA; RNA dimerization; protease; human immunodeficiency virus Type 1; palindrome; zinc finger; tRNA placement; RNA–RNA interactions.

INTRODUCTION

Nucleocapsid protein (NC) of human immunodeficiency virus Type 1 (HIV-1) facilitates RNA–RNA, RNA–protein, and protein–protein interactions such as $tRNA_{Lys3}$ genomic placement (i.e., the *in vivo* placement of primer $tRNA_{Lys3}$ on the primer binding site, as assayed by the incorporation of CTGCTA into intraviral $tRNA_{Lys3}$ in the presence of dTTP, dCTP, dGTP, ddATP, and exogenous HIV-1 reverse transcriptase), $tRNA_{Lys3}$ and genomic RNA encapsidation, the initiation and elongation steps of proviral DNA synthesis, and p55gag multimerization and incorporation of p160gag-pol into viruses. These functions are differentially affected by the subdomains of NC, which are the N-terminus (residues 1–13, a basic region), F1 (or the proximal Zn knuckle: residues 14–30), the linker (residues 31–34, a strongly basic region), F2 (or the distal Zn knuckle: residues 35–51), and the C-terminus (residues 52–55, or 52–71 prior to proteolytic cleavage into NCp7 and protein p1) (Morellet *et al.,* 1994; Summers *et al.,* 1992). For example, F2 facilitates genome packaging (Cen *et al.,* 1999; Gorelick *et al.,* 1990; Zhang and Barklis, 1995) and 2-base extension of $tRNA_{Lys3}$ (Huang *et al.,* 1998) rather than viral incorporation or genomic placement of $tRNA_{Lys3}$ (Huang *et al.,* 1997a, 1998); the basic residues of the linker facilitate genome packaging (Cen *et al.,* 1999; Ottmann *et al.,* 1995) and $tRNA_{Lys3}$ placement (Huang *et al.,* 1998) rather than $tRNA_{Lys3}$ incorporation (Huang *et al.,* 1997a) and 2-base extension of $tRNA_{Lys3}$ (Huang *et al.,* 1998); Pro31 facilitates $tRNA_{Lys3}$ packaging, via stimulating viral incorporation of p160gag-pol (Huang *et al.,* 1997a), but has no impact on genome packaging (Ottmann *et al.,* 1995). This is summarized in the last four columns of Table 1. Zn knuckles, also called Zn fingers or Cys-His boxes, are CCHC-type structures (Cys-X2-Cys-X4-His-X4-Cys, where X = variable amino acid) bearing a limited resemblance to the CCHH-type Zn fingers found in eukaryotic transcription factors.

A dimeric HIV genome appears essential for viral in-

[1] To whom reprint requests should be addressed at Lady Davis Institute for Medical Research, 3755 Cote Ste. Catherine Road, Montreal, Quebec, Canada H3T 1E2. Fax: (514) 340-7502. E-mail: laughrea@hotmail.com or mdla@musica.mcgill.ca.

0042-6822/01 $35.00

fectivity (Shen *et al.,* 2000). Though genomic RNA isolated from protease-defective HIV-1 is known to be less dimeric and less thermostable than wild-type (Fu *et al.,* 1994), no one knows if NC facilitates HIV genomic RNA dimerization. In the first part of this paper, we investigate the effects of various NC mutations on genomic RNA dimerization within isolated HIV-1 viruses. Our goal is to test if NC mutations can prevent genomic RNA dimerization *in vivo*, and, if so, to identify which NC subdomains appear involved and which appear uninvolved.

Electron microscopic characterization of genomic RNA isolated from HIV-1 shows that the two strands of dimeric genomic RNA are linked near their 5′ ends at two points separated by 161 ± 22 nts, the upstream linkage point being such that free 5′ ends cannot be visualized. Combining this information with computer modeling revealed that a single stable structure was consistent with the electron microscopic data. This structure originates from loop–loop interactions between the AAGCUU82 palindromes of two adjacent R-U5 hairpins and the GCGCGC262 (or GUGCAC262) palindromes of two adjacent kissing-loop domains (KLD or SL1) (Hoglund *et al.,* 1997). [The KLD (Clever and Parslow, 1997; Laughrea *et al.,* 1999; McBride and Panganiban, 1997; Shen *et al.,* 2000, and references therein) and the R-U5 hairpin (Berkhout *et al.,* 1997; Clever *et al.,* 1999; Klasens *et al.,* 1998; McBride *et al.,* 1997) are well defined at the secondary structure level. In the HIV-1_{Lai}/HIV-1_{Hxb2}/BH10 isolates, their respective sequences are 243CUCGGCUUGCUGAA**GCGCGC**ACGGCAAGAGGCGAG277 and 58CACUGCUUAAGCCUCAAUA**AAGCUU**GCCUUGAGUGCUUCAAGUAGUG104 (palindromes in bold and stem-forming nts underlined); the two palindromes are separated by 179 nts.] These initial contacts would be followed by more substantial intermolecular hydrogen bonding via switching of the respective stems from intra- to interstrand base-pairing. In the second part of this paper, we verify that disrupting the palindrome of the R-U5 hairpin reduces genomic RNA dimerization in otherwise wild-type viruses or in viruses which already harbor a destroyed KLD or a destroyed kissing-loop hairpin. [The kissing-loop (or DIS) hairpin is nts 248–270. Destroying the KLD, the kissing-loop hairpin, or the palindrome of the kissing-loop hairpin reduces genomic RNA dimerization by ~50% (Clever and Parslow, 1997; Laughrea *et al.,* 1997; Shen *et al.,* 2000), and viral replication by 1.4 to 4 logs depending on the nature of the mutation (Shen *et al.,* 2000).]

RESULTS

Effect of NC mutations on genomic RNA dimerization

Seven NC mutations were inserted in the pNL4–3 HIV-1 molecular clone: R7R10K11S, P31L, R32G, S3(32–34), K59L, C15S/C18S, and C36S/C39S. [NC sequence: IQKGNF**R**NQ**RK**TVK**C**FN**C**GKEGHIAKNCRA**PRKK**G**C**WK**C**GKEGHQWKDCTERQANFLG**K**IWPSHKGRPGNF71 (mutated residues in bold; Zn knuckles underlined).] In R7R10K11S, Arg7, Arg10, and Lys11 have each been replaced by Ser; in S3(32–34), ArgLysLys34 has been replaced by SerSerSer34. The other mutations are self-explanatory. The importance of many of these mutations can be appreciated from inspecting the NMR structure of NCp7 bound to the SL3 RNA stem-loop (nts 312–325) in the HIV-1 packaging signal (De Guzman *et al.,* 1998). The 5-bp stem interacted with Arg7, Arg10, and Lys11 via nonspecific electrostatic interactions. The GGAG320 tetraloop interacted with F1, the linker, and F2: for example, A319 was hydrogen-bonded to Arg32 while G318 bound to a hydrophobic cleft in F2; Lys47 projected between the two phosphodiesters flanking G318, easing repulsion and anchoring F2 to the RNA. The linker had a very stable conformation: Arg32 was hydrogen-bonded to F1 while Pro31 and Lys33 were, respectively, hydrogen-bonded to F1 and F2 (De Guzman *et al.,* 1998).

COS-7 cells were transfected in parallel with equal amounts of pSVC21.BH10 or mutant plasmids (Materials and Methods). To investigate the effects of the mutations on genome dimerization, genomic RNA was extracted from the isolated viruses, electrophoresed on a nondenaturing agarose gel, and visualized by Northern blotting with a ^{35}S-labeled HIV-1 riboprobe (Materials and Methods). Infectious molecular clones pSVC21.BH10 and pNL4–3 contain essentially identical (Korber *et al.,* 1997) subtype B wild-type HIV-1 proviral DNAs (Levy *et al.,* 1986; Terwillinger *et al.,* 1989). Both clones yield viruses containing ~85% dimeric genomic RNA (Haddrick *et al.,* 1996; Laughrea *et al.,* 1997; Shen *et al.,* 2000). Figure 1 presents genomic RNAs from BH10 and six of the seven NC mutants. [C15S/C18S, perhaps because it packages genomic RNA ~25 times more poorly than wild-type (Cen *et al.,* 1999; Gorelick *et al.,* 1990), did not yield sufficiently clean Northern blots (not shown).] Genomic RNAs from protease-defective (PR^-) viruses (lane 7) and viruses mutated in the kissing-loop palindrome (lane 10) or grown in the presence of the protease inhibitor Saquinavir (lane 6) are also presented for comparison. Scanning lanes 1–8 and 11 (and other lanes representing two to three additional independent transfections per mutant, e.g., lane 8 of Fig. 2) reveals that genomic RNAs isolated from BH10, R7R10K11S, S3(32–34), R32G, P31L, and K59L viruses were, respectively, 84 ± 2, 77 ± 5, 78 ± 3, 82.5 ± 6, 76 ± 6, and 88 ± 4% dimeric. PR^- viruses and viruses isolated from Saquinavir-treated cells had genomic RNAs which were, respectively, 19 ± 5 and 30 ± 6% dimeric. Scanning lanes 9–10 (and other cognate lanes representing three independent transfections per mutant) reveals that UUAA261 and C36S/C39S genomic RNAs were, respectively, 55 ± 4 (Shen *et al.,* 2000) and 49 ± 5% dimeric. Thus disrupting F2 inhibited genome dimerization as much as replacing the GCGCGC262 palindrome with the weaker GUUAAC262

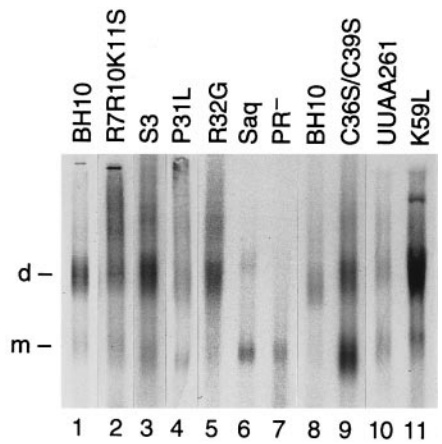

FIG. 1. Dimerization level of viral RNA isolated from BH10, R7R10K11S, S3(32–34), P31L, R32G, protease-defective (lane 7), C36S/C39S, kissing-loop inactivated [lane 10; see Shen *et al.* (2000)], and K59L viruses; saq (lane 6) represents BH10 viruses obtained after transfection in the presence of 0.4 μM Saquinavir. Saquinavir was a gift from R. Germinario. In PR$^-$, defined in Table 1, proteolytic cleavage of p55gag and p160gag-pol is abolished (Gottlinger *et al.,* 1989; Le Grice *et al.,* 1988; Loeb *et al.,* 1989). Viral RNAs were dissolved in 8 μl of buffer S and subjected to electrophoresis for 4 h 30 min (5 h for lanes 3–9). The samples were next Northern blotted, hybridized, and autoradiographed for 45 min to 12 h. d, dimer; m, monomer. Each lane represents an independent transfection and contains viral RNA isolated from 3 to 20 tissue culture dishes. The respective percentages of dimerization in lanes 1–11 are 82, 77, 78, 73, 89, 31, 18, 81, 46, 57, and 90% dimeric. On average, UUAA viruses are 55 ± 4% dimeric (Shen *et al.,* 2000; Table 1).

[or disrupting the palindrome via a C258G transversion (Shen *et al.,* 2000)] but less than inactivating the viral protease or treating the transfected cells with a protease-inhibitor; mutating the N-terminal, linker, or C-terminal subdomains of NC was ineffective.

Effect of the palindrome crowning the R-U5 hairpin on genomic RNA dimerization

COS-7 cells were transfected with equal amounts of pSVC21.BH10 and mutant plasmids such as pSVC21Δ248–261, Δ241–256, Δ78–81, Δ78–81/Δ248–261, Δ78–81/Δ241–256, and $(AGCU81)_2$/Δ248–261 (Materials and Methods). Lanes 1–4 of Fig. 2 compare genomic RNAs from Δ78–81 and BH10 viruses. Scanning these lanes, as well as many other gel lanes from independent transfections, reveals that Δ78–81 and BH10 genomic RNAs were, respectively, 84 ± 4 and 84 ± 2% dimeric. An *in vitro* dimerization signal 3′ of the KLD is concealed when the KLD bears a "strong" GCGCGC or GGGCCC palindrome and revealed when it bears a "weak" GUGCAC or GUGCGC palindrome (Laughrea and Jetté, 1997; Laughrea *et al.,* 1999; Paillart *et al.,* 1994). Thus the palindrome of the R-U5 hairpin might conceivably make a contribution to genome dimerization which is concealed (or hard to detect) when the KLD is functional. Accordingly, genomic RNA from Δ78–81/Δ241–256 viruses was compared to that of control Δ241–256 viruses. Both viruses bear an inactivated KLD (Shen *et al.,* 2000). Lanes 5–7 of Fig. 2 show that Δ78–81/Δ241–256 genomic RNA was as dimeric as Δ241–256 genomic RNA. Scanning lanes 5 to 7, as well as many other gel lanes from independent transfections, reveals that Δ78–81/Δ241–256 and Δ241–256 genomic RNAs were, respectively, 44 ± 3 and 45 ± 4% dimeric. Δ248–261, Δ78–81/Δ248–261, and $(AGCU81)_2$/Δ248–261 genomic RNAs were also compared: they were, respectively, 36 ± 4, 29 ± 4, and 39 ± 4% dimeric (not shown). In addition, the dissociation temperature of these three RNAs was found to be 48–50°C, independent of the mutation (not shown).

DISCUSSION

NC requirements for genome dimerization and $tRNA_{Lys3}$ placement appear diametrically different but are not

The genomic RNA dimerization data presented here contribute to our ongoing study of the role of NC in functions which have included genome packaging (Cen *et al.,* 1999; Ottmann *et al.,* 1995), viral incorporation of p160gag-pol and $tRNA_{Lys3}$ (Huang *et al.,* 1997a), genomic placement, and 2-base extension of $tRNA_{Lys3}$ (Huang *et al.,* 1998). To maximize insights, all of these studies investigated identically mutated viruses produced and

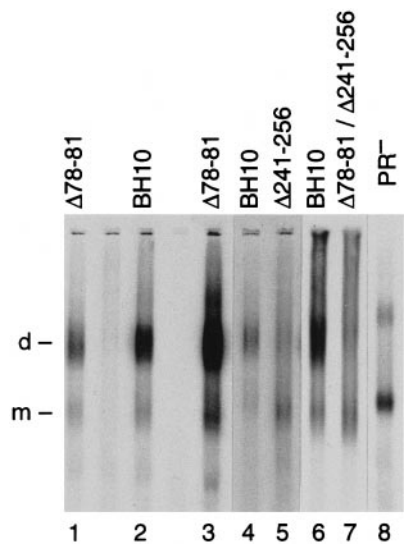

FIG. 2. Dimerization level of viral RNA isolated from BH10, Δ78–81, Δ241–256, Δ78–81/Δ241–256, and PR$^-$ viruses. Viral RNAs were dissolved in 8 μl of buffer S and subjected to electrophoresis for 4 h 30 min. The samples were next Northern blotted, hybridized, and autoradiographed for 8 h (lanes 1–3), 20 min (lanes 4–5), 25 h (lanes 6–7), and 4 h (lane 8). d, dimer; m, monomer. Each lane represents an independent transfection and contains viral RNA isolated from 4 to 10 tissue culture dishes. Lanes 1–7 represent viral RNA isolated from viruses containing, respectively, 5, 15, 40, 300, 300, 6 and 14 × 10^{10} CAp24. Different transfections were used to produce the PR$^-$ genomic RNAs presented in lane 8 and in lane 6 of Fig. 1.

TABLE 1

Effect of NC Mutations on Genomic RNA Dimerization, Genomic RNA Packaging, Genomic Placement of $tRNA_{Lys3}$, Viral Incorporation of $tRNA_{Lys3}$, and 2-Base Extension of $tRNA_{Lys3}$ Inside Isolated HIV-1 Viruses

Virus	Genomic RNA dimerization	Genomic RNA packaging	Genomic placement[a] (and incorporation[b]) of $tRNA_{Lys3}$	2-Base extension of placed $tRNA_{Lys3}$[a]
Wild-type	100	100	100 (+)	100
R7R10K11S	92 ± 6	*~30*[c,d,e]	*24* (+)	75
C15S/C18S	?	*2*[f] to *6*[c]	54 (+)	*50*
P31L	90 ± 7	100[g]	*7* (−)	Not detected
R32G	99 ± 6	*15*[g]	*19* (+)	122
S3(32–34)	93 ± 4	*20*[c,e,h]	*25* (+)	114
C36S/C39S	*58* ± *6*	*22*[c,f]	105 (+)	*69*
K59L	105 ± 6	40[b]	87 (+)	99
PR^-	*19* ± *5*[i]	100	~100[j] (+)[k]	*<5*[i]
UUAA	*65* ± *5*[l]			
Δ248–261 and Δ248–256	*51* ± *5*[l]			

[a] From Huang *et al.* (1998). Last column: proportion of placed $tRNA_{Lys3}$ which was already 2-base extended in the isolated viral RNA. 80% of placed $tRNA_{Lys3}$ was already 2-base extended in isolated wild-type viral RNA: this was scored as 100; 60% of placed $tRNA_{Lys3}$ was already 2-base extended in R7K10K11 viral RNA: this was scored as 75, etc. P31L prevented packaging of p160gag-pol and processing of p55gag.

[b] From Huang *et al.* (1997a). Incorporation describes the selective packaging of $tRNA_{Lys}$ inside virions, which itself depends on viral incorporation of p160Gag-pol (Mak *et al.,* 1994). +, −: $tRNA_{Lys}$ represents, respectively, 50–60% or 5–6% of low-molecular-weight viral RNA.

[c] From Cen *et al.* (1999).

[d] From Berthoux *et al.* (1997).

[e] R10K11A and R29R32K33K34A respectively yielded a 32 and 14% genomic RNA packaging efficiency (Poon *et al.,* 1996).

[f] From Gorelick *et al.* (1990). C15S and C18S yielded a 10–15% genomic RNA packaging efficiency (Dorfman *et al.,* 1993); C15Y/C18Y/C36Y/C39Y yielded an ~25% genomic RNA packaging efficiency (Zhang and Barklis, 1995).

[g] From Ottmann *et al.* (1995).

[h] R32K33K34E yielded a 12% genomic RNA packaging efficiency (Sheng *et al.,* 1997).

[i] $SVC21PR^-$ differs from SVC21.BH10 by the conversion of Asp25 into Arg25 in the protease coding region (Gottlinger *et al.,* 1989). Fu *et al.* (1994) had reported a ~50% inhibition of genome dimerization with a PR^- clone having Asp25 converted into Ala25. Each of these mutations abolish proteolytic cleavage of p55gag and p160gag-pol (Gottlinger *et al.,* 1989; Le Grice *et al.,* 1988; Loeb *et al.,* 1989).

[j] From Huang *et al.* (1997b).

[k] From Mak *et al.* (1994).

[l] From Shen *et al.* (2000).

purified using essentially identical protocols (Cen *et al.,* 1999; Huang *et al.,* 1997a, 1998; Ottmann *et al.,* 1995; present data). Table 1 summarizes present data (first column) and our previously published results (remaining columns). Two of the functions studied ($tRNA_{Lys3}$ genomic placement and genomic RNA dimerization) represent RNA–RNA interactions. Yet they appear to have diametrically different NC requirements. We suggest that reality is otherwise, for two reasons. First, it is now known [but was not at the time of Huang *et al.* (1998)] that there are two kinds of $tRNA_{Lys3}$ placement. Immature placement allows nonprocessive nt polymerization (tRNA extension stalls after addition of 3 to 10 nts) and is not dramatically inhibited by deletion of both Zn knuckles (Rong *et al.,* 1998); mature placement allows synthesis of minus-strand strong stop DNA but does not tolerate destruction of the Zn knuckles (Rong *et al.,* 1998). The placement assay of Table 1 therefore detected both immature and mature tRNA placement because it measured the ability of intraviral $tRNA_{Lys3}$ to be extended 6 nts by *in vitro* reverse transcription (Introduction; Huang *et al.,* 1998). Second, some of this $tRNA_{Lys3}$ had already been extended 2 bases inside the virus (Huang *et al.,* 1998; Table 1). If this intraviral 2-base extension assayed mature tRNA placement, then NC requirements for the two RNA–RNA interactions inside HIV-1 would become closely related (Table 1). Supporting this view, *in vitro* experiments have implicated W37 in NCp7-directed annealing of $tRNA_{Lys3}$ to the primer binding site (Remy *et al.,* 1998). If NCp7-driven tRNA annealing and RNA dimerization are related activities, Trp37 should stimulate NCp7-driven RNA dimerization: W37A slows down the maturation of a dimeric partial transcript from Harvey sarcoma virus (Feng *et al.,* 1996), implicating the distal Zn knuckle in an annealing process which may resemble HIV-1 genomic RNA dimerization. We infer that mature tRNA placement and *in vivo* genome dimerization are directed by NCp7 (PR^- row of Table 1 shows little activity) via the sequence-specific RNA binding activity of its Zn knuckles, rather than via the phosphodiester neutralizing function of its linker and N-terminus (fourth and first columns of Table 1). [It was previously thought that NCp7-promoted RNA dimerization and hybridization of $tRNA_{Lys3}$ to genomic RNA was independent of the Zn knuckles and

dependent on the linker and N-terminal subdomains (De Rocquigny *et al.,* 1992).]

Comparison with other retroviruses

Our finding that the N-terminal and linker subdomains of NC play no role in HIV-1 genome dimerization supports analogous experiments with Moloney murine leukemia virus (MMLV), where neutralizing the basic amino acids flanking the Zn knuckle (via mutations RRR18LSS or KK42TI) had no impact on genome dimerization, even though it reduced genome packaging by 90–95% (Housset *et al.,* 1993). Our finding that the distal Zn knuckle plays a key role in genome dimerization supports previous experiments with Rous sarcoma virus (RSV), where disrupting the proximal or distal Zn knuckle, or interchanging them, reduced genome dimerization by ~50%, though most point mutations had no effect (Bowles *et al.,* 1993; Dupraz *et al.,* 1990; Méric and Spahr, 1986; Méric *et al.,* 1988). (The effect of neutralizing basic NC residues was not studied in RSV.) Even though key point mutations in the MMLV Zn knuckle, such as Y28G and W35L (which reduced genome packaging by 96 to 98%) and C39H (which blocked viral replication without reducing packaging), had no effect on genome dimerization (Gorelick *et al.,* 1988, 1999; Méric and Goff, 1989), we infer from the RSV/HIV results and the nonimplication of RRR18 and KK42 in MMLV genome dimerization that the MMLV Zn knuckle probably plays a role in genome dimerization. It will be interesting to search for the implicated residue(s). Perhaps emphasizing this apprehended exquisite versatility of the single Zn knuckle of MMLV, Y28, H34, and C39 of NCp10 make contacts with nonknuckle residues the equivalent of which does not exist in NCp7 (Déméné *et al.,* 1994).

On the AAGCUU82 palindrome

Since the palindrome crowning the R-U5 hairpin had no significant impact on the dimerization of genomic RNA isolated from HIV-1, the 5′ dimerization signal identified by electron microscopy is unlikely to exist under physiological conditions. This is congruent with the observation that destruction of the R-U5 hairpin did not impact the dimerization of partial HIV-1 RNA transcripts (Laughrea and Jetté, 1996). Since inactivating both palindromes of the R-U5 and kissing-loop hairpins left at least 30% of genomic RNA in a dimeric state, significant dimerization signals appear to be located outside these hairpins. The variant results obtained by microscopic characterization can be explained as follows. To spread the otherwise tightly coiled RNA molecules on electron microscopy grids, it was necessary to partially denature them in urea and formamide (Hoglund *et al.,* 1997). This treatment may have had complex effects on RNA structure, such as a mixture of general uncoiling/unwinding and local redistribution of the base-pairing pattern artificially favoring dimerization at the level of the R-U5 hairpin.

MATERIALS AND METHODS

Buffers and media

Buffer S consisted of 10 mM Tris (pH 7.5), 100 mM NaCl, 1 mM EDTA, and 1% SDS (Fu *et al.,* 1994). Buffer TBE_2 consisted of 89 mM Tris, 89 mM borate, and 2 mM EDTA. R-10 medium was R-20 medium (Laughrea *et al.,* 1997) with 10% fetal bovine serum (Gibco) and without Hepes.

Plasmid construction

Plasmid pSVC21.BH10 encodes an infectious HIV-1_{Hxb2} clone derived from the IIIB strain of HIV-1 (Laughrea *et al.,* 1997). To create the nucleocapsid (NC) mutations, site-directed mutagenesis was carried out as previously described (Gorelick *et al.,* 1990; Ottman *et al.,* 1995). NC mutants C15S/C18S and C36S/C39S were donated by A. Rein and R. Gorelick.

R-U5 hairpin mutations were introduced into three control plasmids: wild-type pSVC21.BH10, mutant pSVC21Δ248–261 (kissing-loop hairpin destroyed), and mutant pSVC21Δ241–256 (kissing-loop domain destroyed). Plasmids pSVC21Δ248–261 and pSVC21Δ241–256 have been described previously (Laughrea *et al.,* 1997; Shen *et al.,* 2000). The palindrome of the R-U5 hairpin was mutated as follows. Plasmid pBL contains the 1–965 region of HIV-1_{Lai} RNA (Laughrea and Jetté, 1994). It was cut with *Xho*I and *Acc*I and recircularized to eliminate the second of its two *Hin*dIII sites. The DNA between the *Hpa*I and Nar I sites was removed and replaced by the *Hpa*I-NarI DNA of SVC21.BH10. Its unique *Hin*dIII site, corresponding to AAGCUU82 in the apical loop of the R-U5 hairpin, was cleaved and treated either with mung bean nuclease or with Klenow polymerase in the presence of deoxynucleoside triphosphates (Sambrook *et al.,* 1989). The DNA was transformed into *Escherichia coli* after ligation of the blunt ends. The *Hpa*I-*Nar*I fragment of the mutated plasmids was cloned into the corresponding sites of pSVC21.BH10, Δ248–261, or Δ241–256 to create mutant plasmids such as pSVC21Δ78–81/Δ248–261, Δ78–81/Δ241–256, and $(AGCU81)_2$/Δ248–261. In pSVC21Δ78–81/Δ248–261, AGCU81 and CUUGCUGAAGCGCG261 have been deleted; in $(AGCU81)_2$/Δ248–261, AGCU has been inserted between U81 and U82 and CUUGCUGAAGCGCG261 has been deleted, mutatis mutandis for the other plasmids. All constructs were sequenced to verify that the correct mutations had been achieved.

Transfections and virus preparation

Transfection of COS-7 cells with the above plasmids by the calcium phosphate method was as previously

described (Huang *et al.,* 1997a, 1998; Laughrea *et al.,* 1997). Old medium (DMEM/fetal calf serum) was removed at 24 h posttransfection; fresh medium (7 ml/dish) was added back to each plate after the cells were washed twice, and viruses were isolated from the cell culture supernatant obtained at 48 h posttransfection. The supernatant was centrifuged in a GS-6R rotor at 3000 rpm for 15 min and passed through a 0.22-μm cellulose acetate filter (Corning). This clarified COS-7 culture supernatant fluid was centrifuged in a Ti45 rotor at 35,000 rpm for 1 h at 4°C. The pellet was dissolved in phosphate-buffered saline (Sambrook *et al.,* 1989) and centrifuged through 4 ml 15% sucrose in phosphate-buffered saline onto a 2-ml 65% sucrose cushion in the same buffer (SW41, 26500 rpm, 1 h, 4°C). The interface, in a 3-ml fraction, was taken and centrifuged 1 h at 40,000 rpm to pellet the virus.

Isolation of HIV-1 genomic RNA

Viruses were disrupted in 0.5–1 ml sterile lysis buffer consisting of 50 mM Tris (pH 7.4), 10 mM EDTA, 1% SDS, 50 mM NaCl, 50 μg of yeast tRNA per milliliter, and 100 μg of proteinase K per milliliter (Laughrea *et al.,* 1997). Resuspended pellets were incubated at 37°C for 30 min and then extracted two times with an equal volume of buffer-saturated phenol–chloroform-isoamyl alcohol (25:24:1, pH 7.5). The aqueous phase, containing the viral RNA, was precipitated in 70% ethanol at −80°C, using 0.3 M sodium acetate (pH 5.2).

Electrophoretic and thermal analysis of HIV-1 genomic RNA

Viral RNA pelleted from ethanol suspension was dissolved in buffer S and analyzed by nondenaturing Northern blot analysis as described previously (Laughrea *et al.,* 1997). Electrophoretic conditions were 70 V on 1% agarose gels in TBE_2 at 4°C for the indicated times. For thermal analysis, the RNAs were incubated at the indicated temperatures for 10 min prior to electrophoresis. The amount of genomic RNA in the gels was quantitated by hybridization with a ^{35}S-labeled antisense RNA 636–296, as described previously (Laughrea *et al.,* 1997). The RNAs were vacuum transferred from the agarose gel to a Hybond N^+ nylon membrane sandwiched within a Hybri-Dot filtration manifold. After drying, cross-linking, and prehybridization, the nylon membrane was hybridized overnight to approximately 10^7 cpm of antisense RNA 636–296. This was followed by three washes and autoradiography. The autoradiograms were scanned with a Supervista S-12 UMAX densitometer and the intensity of the dimer band was measured as a proportion of the total intensity of the dimer and monomer bands. Margins or errors represent the standard deviation obtained after pooling of the results from at least three independent transfections. Each scan covered the full length of each lane to correctly establish the baseline from which monomer and dimer peak areas were quantitated.

Physical virus titer

The physical virus titer was determined by estimating the amount of capsid protein (CAp24) in purified viruses or in clarified COS-7 culture supernatant fluid (Laughrea *et al.,* 1997). CAp24 was estimated using a p24 enzyme-linked immunosorbent assay detection kit (Abbott Laboratories) according to the manufacturer's recommendations.

Genomic RNA packaging assay

Assuming that mutant and wild-type viruses contain on average the same quantity of CAp24 per particle, genomic RNA packaging was derived from the scans of the Northern blots: the intensity of the mutant RNA profiles relative to BH10 was normalized according to the amount of mutant CAp24 loaded relative to BH10.

Infectivity assay

The number of 50% tissue culture infective doses ($TCID_{50}$) contained in a mutant and a wild-type viral preparation was measured in two 96-well flat-bottom plates as previously described (Laughrea *et al.,* 1997), except that R-10 medium was used in place of R-20 medium. Each experiment was done in octuplicate (Laughrea *et al.,* 1997).

ACKNOWLEDGMENT

This work was supported by a grant (MT-12312) from the Medical Research Council of Canada to Michael Laughrea.

REFERENCES

Berkhout, B., Klaver, B., and Das, A. T. (1997). Forced evolution of a regulatory RNA helix in the HIV-1 genome. *Nucleic Acids Res.* **25,** 940–947.

Berthoux, L., Péchoux, C., Ottmann, M., Morel, G., and Darlix, J. L. (1997). Mutations in the N-terminal domain of human immunodeficiency virus type 1 nucleocapsid protein affect virion core structure and proviral DNA synthesis. *J. Virol.* **71,** 6973–6981.

Bowles, N. E., Damay, P., and Spahr, P.-F. (1993). Effect of rearrangements and duplications of the Cys-His motifs of Rous Sarcoma virus nucleocapsid protein. *J. Virol.* **67,** 623–631.

Cen, S., Huang, Y., Khorchid, A., Darlix, J.-L., Wainberg, M. A., and Kleiman, L. (1999). The role of $Pr55^{gag}$ in the annealing of $tRNA_{Lys3}$ to Human Immunodeficiency Virus Type 1 genomic RNA. *J. Virol.* **73,** 4485–4488.

Clever, J. L., and Parslow, T. G. (1997). Mutant human Immunodeficiency Virus Type 1 genomes with defects in RNA dimerization or encapsidation. *J. Virol.* **71,** 3407–3414.

Clever, J. L., Eckstein, D. A., and Parslow, T. G. (1999). Genetic dissociation of the encapsidation and reverse transcription functions in the 5′ R region of human immunodeficiency virus Type 1. *J. Virol.* **73,** 101–109.

De Guzman, R. N., Wu, Z. R., Stalling, C. C., Pappalardo, L., Borer, P. N., and Summers, M. F. (1998). Structure of the HIV-1 nucleocapsid

protein bound to the SL3 psi-RNA recognition element. *Science* **279,** 384–388.

Déméné, H., Jullian, N., Morellet, N., De Rocquigny, H., Cornille, F., Maigret, B., and Roques, B. P. (1994). Three-dimensional ^{1}H NMR structure of the nucleocapsid protein NCp10 of Moloney murine leukemia virus. *J. Biomol. NMR* **4,** 153–170.

De Rocquigny, H., Gabus, C., Vincent, A., Fournié-Zaluski, M.-C., Roques, B. P., and Darlix, J.-L. (1992). Viral RNA annealing activities of human imunodeficiency virus type 1 nucleocapsid protein require only peptide domains outside the zinc fingers. *Proc. Natl. Acad. Sci. USA* **89,** 6472–6476.

Dorfman, T., Luban, J., Goff, S. P., Haseltine, W. A., and Gottlinger, H. G. (1993). Mapping of functionally important residues of a cysteine-histidine box in the human immunodeficiency virus Type 1 nucleocapsid protein. *J. Virol.* **67,** 6159–6169.

Dupraz, P., Oertle, S., Méric, C. Damay, P., and Spahr, P.-F. (1990). Point-mutations in the proximal Cys-His box of Rous sarcoma virus nucleocapsid protein. *J. Virol.* **64,** 4978–4987.

Feng, Y.-X., Copeland, T. D., Henderson, L. E., Gorelick, R. J., Bosche, W. J., Levin, J. G., and Rein, A. (1996). HIV-1 nucleocapsid protein induces "maturation" of dimeric retroviral RNA *in vitro*. *Proc. Natl. Acad. Sci. USA* **93,** 7577–7581.

Fu, W., Gorelick, R. J., and Rein, A. (1994). Characterization of human immunodeficiency virus Type 1 dimeric RNA from wild-type and protease-defective virions. *J. Virol.* **68,** 5013–5018.

Gorelick, R. J., Henderson, L. E., Hanser, J. P., and Rein, A. (1988). Point mutants of Moloney murine leukemia virus that fail to package viral RNA: Evidence for specific RNA recognition by a "zinc finger-like" protein sequence. *Proc. Natl. Acad. Sci. USA* **85,** 8420–8424.

Gorelick, R. J., Nigida, Jr., S. M., Bess, Jr., J. W., Arthur, L. O., Henderson, L. E., and Rein, A. (1990). Noninfectious human immunodeficiency virus Type 1 mutants deficient in genomic RNA. *J. Virol.* **64,** 3207–3211.

Gorelick, R. J., Fu, W., Gagliardi, T. D., Bosche, W. J., Rein, A., Henderson, L. E., and Arthur, L. O. (1999). Characterization of the block in replication of Nucleocapsid protein zinc finger mutants from Moloney murine leukemia virus. *J. Virol.* **73,** 8185–8195.

Gottlinger, H. E., Sodroski, J. G., and Haseltine, W. A. (1989). Role of capsid precursor processing and myristoylation in morphogenesis and infectivity of human immunodeficiency virus Type 1. *Proc. Natl. Acad. Sci. USA* **86,** 5781–5785.

Haddrick, M., Lear, A. L., Cann, A. J., and Heaphy, S. (1996). Evidence that a kissing loop structure facilitates genomic RNA dimerization in HIV-1. *J. Mol. Biol.* **259,** 58–68.

Hoglund, S., Ohagen, A., Goncalves, J., Panganiban, A. T., and Gabuzda, D. (1997). Ultra-structure of HIV-1 genomic RNA. *Virology* **233,** 271–279.

Housset, V., De Rocquigny, H., Roques, B. P., and Darlix, J.-L. (1993). Basic amino acids flanking the zinc finger of Moloney murine leukemia virus nucleocapsid protein NCp10 are critical for virus infectivity. *J. Virol.* **67,** 2537–2545.

Huang, Y., Khorchid, A., Wang, J., Parniak, M. A., Darlix, J.-L., Wainberg, M. A., and Kleiman L. (1997a). Effect of mutations in the nucleocapsid protein (NCp7) upon $Pr160^{gag\text{-}pol}$ and $tRNA_{Lys}$ incorporation into Human Immunodeficiency Virus Type 1. *J. Virol.* **71,** 4378–4384.

Huang, Y., Wang, J., Shalom, A., Li, Z., Khorchid, A., Wainberg, M. A., and Kleiman, L. (1997b). Primer tRNA Lys3 on the viral genome exists in unextended and two-base extended forms within mature human immunodeficiency virus Type 1. *J. Virol.* **71,** 726–728.

Huang, Y., Khorchid, A., Gabor, J., Wang, J., Li, X., Darlix, J.-L., Wainberg, M. A., and Kleiman, L. (1998). The role of nucleocapsid and U5/A-rich loop sequences in $tRNA_{Lys3}$ genomic placement and initiation of reverse transcription in human immunodeficiency virus Type 1. *J. Virol.* **72,** 3907–3915.

Klasens, B. I. F., Das, A. T., and Berkhout, B. (1998). Inhibition of polyadenylation by stable RNA secondary structure. *Nucleic Acids Res.* **26,** 1870–1878.

Korber, B., Hahn, B., Foley, B., Mellors, J. W., Leitner, T., Myers, G., McCutchan, F., and Kuiken, C., Eds. (1997). "Human Retroviruses and AIDS 1997." Los Alamos National Laboratory, Los Alamos, NM.

Laughrea, M., and Jetté, L. (1994). A nineteen nucleotide sequence upstream of the 5′ major splice donor is part of the dimerization domain of the HIV-1 genome. *Biochemistry* **33,** 13464–13475.

Laughrea, M., and Jetté, L. (1996). HIV-1 genome dimerization: Formation kinetics and thermal stability of dimeric $HIV\text{-}1_{Lai}$ RNAs are not improved by the 1–232 and 296–790 regions flanking the kissing-loop domain. *Biochemistry* **35,** 9366–9374.

Laughrea, M., and Jetté, L. (1997). HIV-1 genome dimerization: Kissing-loop hairpin dictates whether nucleotides downstream of the 5′ splice junction contribute to loose and tight dimerization of human immunodeficiency virus RNA. *Biochemistry* **36,** 9501–9508.

Laughrea, M., Jetté, L., Mak, J., Kleiman, L., Liang, C., and Wainberg, M. A. (1997). Mutations in the kissing-loop hairpin of human immunodeficiency virus Type 1 reduce viral infectivity as well as genomic RNA packaging and dimerization. *J. Virol.* **71,** 6003–6010.

Laughrea, M., Shen, N., Jetté, L., and Wainberg, M. A. (1999). Variant effects of non-native kissing-loop hairpin palindromes on HIV replication and HIV RNA dimerization; Role of stem-loop B in HIV replication and HIV RNA dimerization. *Biochemistry* **38,** 226–234.

Le Grice, S. F. J., Mills, J., and Mous, J. (1988). Active site mutagenesis of the AIDS virus protease and its alleviation by *trans* complementation. *EMBO J.* **7,** 2547–2553

Levy, J. A., Cheng, M. C., Dina, D., and Luciw, P. A. (1986). AIDS retrovirus (ARV-2) clone replicates in transfected human and animal fibroblasts. *Science* **232,** 998–1001.

Loeb, D. D., Hutchison C. A., III, Edgell, M. H., Farmerie, W. G., and Swanstrom, R. (1989). Mutational analysis of human immunodeficiency virus Type 1 protease suggests functional homology with aspartic proteinases. *J. Virol.* **63,** 111–121.

Mak, J., Jiang, M., Wainberg, M. A., Hammarskjold, M.-L., Rekosh, D., and Kleiman, L. (1994). Role of $Pr160^{gag\text{-}pol}$ in mediating the selective incorporation of $tRNA^{Lys}$ into human immunodeficiency virus Type 1 particles. *J. Virol.* **68,** 2065–2072.

McBride, M. S., and Panganiban, A. T. (1997). Position dependence of functional hairpins important for human immunodeficiency virus Type 1 RNA encapsidation *in vivo*. *J. Virol.* **71,** 2050–2058.

McBride, M. S., Schwartz, M. D., and Panganiban, A. T. (1997). Efficient encapsidation of human immunodeficiency virus Type 1 vectors and further characterization of cis elements required for encapsidation. *J. Virol.* **71,** 4544–4554.

Méric, C., and Spahr, P.-F. (1986). Rous sarcoma virus nucleic acid-binding protein p12 is necessary for viral 70S RNA dimer formation and packaging. *J. Virol.* **60,** 450–459.

Méric, C., and Goff, S. P. (1989). Characterization of Moloney murine leukemia virus mutants with single-amino-acid substitutions in the Cys-His box of the nucleocapsid protein. *J. Virol.* **63,** 1558–1568.

Méric, C., Gouilloud, E., and Spahr, P.-F. (1988). Mutations in Rous sarcoma virus nucleocapsid protein p12 (NC): Deletions of Cys-His boxes. *J. Virol.* **62,** 3328–3333.

Morellet, N., De Rocquigny, H., Mély, Y., Jullian, N., Déméné, H., Ottmann, M., Gérard, D., Darlix, J.-L., Fournié-Zaluski, M. C., and Roques, B. P. (1994). Conformational behaviour of the active and inactive forms of the nucleocapsid NCp7 of HIV-1 studied by ^{1}H NMR. *J. Mol. Biol.* **235,** 287–304.

Ottmann, M., Gabus, C., and Darlix, J.-L. (1995). The central globular domain of the nucleocapsid protein of human immunodeficiency virus type 1 is critical for virion structure and infectivity. *J. Virol.* **69,** 1778–1784.

Paillart, J.-C., Marquet, R., Skripkin, E., Ehresmann, B., and Ehresmann, C. (1994). Mutational analysis of the bipartite dimer linkage structure of human immunodeficiency virus Type 1 genomic RNA. *J. Biol. Chem.* **269,** 27486–27493.

Poon, D. T. K., Wu, J., and Aldovini, A. (1996). Charged amino acid residues of human immunodeficiency virus Type 1 nucleocapsid p7

protein involved in RNA packaging and infectivity. *J. Virol.* **70,** 6607–6616.

Remy, E., De Rocquigny, H., Petitjean, P., Muriaux, D., Theilleux, V., Paoletti, J., and Roques, B. P. (1998). The annealing of tRNALys3 to human immunodeficiency virus Type 1 primer binding site is critically dependent on the NCp7 Zinc finger structure. *J. Biol. Chem.* **273,** 4819–4822.

Rong, L., Liang, C., Hsu, M., Kleiman, L., Petitjean, P., De Rocquigny, H., Roques, B. P., and Wainberg, M. A. (1998). Roles of the human immunodeficiency virus Type 1 nucleocapsid protein in annealing and initiation versus elongation in reverse transcription of viral negative-strand strong-stop DNA. *J. Virol.* **72,** 9353–9358.

Sambrook, J., Fritsch, E. F., and Maniatis, T. (1989). "Molecular Cloning, a Laboratory Manual." Cold Spring Harbor Laboratory Press, Cold Spring Harbor, NY.

Shen, N., Jetté, L., Liang, C., Wainberg, M. A., and Laughrea, M. (2000). Stem-loop B stimulates HIV-1 genomic RNA dimerization, and reverse transcription as much as the DIS hairpin; dissociating genome dimerization from genome packaging; impact of genome dimerization on viral infectivity. *J. Virol.* **74,** 5729–5735.

Sheng, N., Pettit, S. J., Tritch, R. J., Ozturk, D. H., Rayner, M. M., Swanstrom, R., and Erickson-Viitanen, S. (1997). Determinants of the human immunodeficiency virus Type 1 p15NC-RNA interaction that affect enhanced cleavage by the viral protease. *J. Virol.* **71,** 5723–5732.

Summers, M. F., Henderson, L. E., Chance, M. R., Bess, J. W., Jr., South, T. L., Blake, P. R., Sagi, I., Perez-Alvarado, G., Sowder, R. C. III, Hare, D. R., and Arthur, L. O. (1992). Nucleocapsid zinc fingers detected in retroviruses: EXAFS studies of intact viruses and the solution-state structure of the nucleocapsid protein from HIV-1. *Protein Sci.* **1,** 563–574.

Terwillinger, E. F., Cohen, E. A., Lu, Y. C., Sodroski, J. G., and Haseltine, W. A. (1989). Functional role of human immunodeficiency virus type 1 Vpu. *Proc. Natl. Acad. Sci. USA* **86,** 5163–5167.

Zhang, Y., and Barklis, E. (1995). Nucleocapsid protein effects on the specificity of retrovirus RNA encapsidation. *J. Virol.* **69,** 5716–5722.